Aquaculture 435 (2015) 265–274

Contents lists available at ScienceDirect

Aquaculture

journal homepage: www.elsevier.com/locate/aqua-online

A genetic linkage map of red drum (*Sciaenops ocellatus*) and comparison of chromosomal syntenies with four other fish species

Christopher M. Hollenbeck [a,*], David S. Portnoy [a,b], John R. Gold [a,b]

[a] Marine Genomics Laboratory, Harte Research Institute, Texas A&M University-Corpus Christi, 6300 Ocean Drive, Corpus Christi, TX 78412, USA
[b] Department of Life Sciences, Texas A&M University-Corpus Christi, 6300 Ocean Drive, Corpus Christi, TX 78412, USA

ARTICLE INFO

Article history:
Received 18 June 2014
Received in revised form 24 July 2014
Accepted 30 August 2014
Available online 6 September 2014

Keywords:
Red drum
Linkage map
Comparative genomics
Microsatellites

ABSTRACT

A genetic linkage map of anonymous and gene-linked microsatellites was generated for red drum, an economically important sciaenid fish cultured for both restoration enhancement and commercial food-fish production. The consensus map, based on linkage data combined from two full-sib families, consisted of 486 total microsatellites (440 anonymous, 46 gene-linked), and spanned 24 linkage groups corresponding to the 24 (haploid) red drum chromosomes. The linkage map generated was used to identify regions of shared synteny between red drum and four other percomorph species for which genome assemblies are available. Considerable synteny was observed between red drum and all four comparison species, and a synteny-based mapping approach was used to putatively localize an additional 80 genes and monomorphic, gene-linked microsatellites within the red drum genome. The genetic linkage map will be a valuable resource for red drum aquaculture, particularly for candidate-gene approaches to identify and map quantitative trait loci.

1. Introduction

Red drum, *Sciaenops ocellatus*, is an estuarine-dependent, sciaenid fish that is cultured for both restoration enhancement of wild populations and commercial production of food fish. The native distribution of the species is throughout the Gulf of Mexico from Tuxpan, Mexico, to southwestern Florida and along the eastern coast of the United States from southeastern Florida to Massachusetts (Pattillo et al., 1997). In response to declines in red drum abundance in the 1980s, red drum restoration-enhancement programs have been implemented in Texas, Florida, Georgia, and South Carolina (McEachron et al., 1995; Smith et al., 2001; Tringali et al., 2008; Woodward, 2000). In China, sciaenid fishes, including red drum, are the largest source of marine finfish fry production (Hong and Zhang, 2003). Globally, commercial production of red drum has risen sharply in recent years, increasing from 2115 tons in 2000 to 67,977 tons in 2012 (http://www.fao.org/fishery/statistics/global-aquaculture-production/query/en).

A central problem in commercial aquaculture is maximizing production efficiency. Genetic improvement of farmed aquatic species has been suggested as a permanent and cumulative solution to this problem (Gjedrem et al., 2012). Most traits targeted by selective breeding programs are influenced by many genes (quantitative trait loci, QTL) with additive effects and/or epistatic interactions (Falconer and Mackay, 1996; Lynch and Walsh, 1998). Genetic marker-based breeding schemes that exploit linkage associations between easily screened genetic markers and QTL offer advantages over traditional breeding programs, particularly for traits that are difficult to measure and for species with relatively long generation times (Hulata, 2001; Sonesson, 2007). Genetic linkage maps of polymorphic markers are a critical first step in establishing marker-based selection programs and also provide a framework for physical mapping and genome assembly (Danzmann and Gharbi, 2007; Liu and Cordes, 2004).

An alternative strategy for identifying QTL is a candidate-gene approach where a priori information about a gene's biological function is used to predict that gene's impact on a trait of interest (Lynch and Walsh, 1998). This approach has been used in fishes to identify QTL affecting spawning time (Leder et al., 2006), growth rate (Sánchez-Molano et al., 2011; Tao and Boulding, 2003), and sex determination (Loukovitis and Sarropoulou, 2012; Shirak et al., 2006). Further, the advent of next-generation DNA sequencing has led to the generation of massive amounts of genetic sequence data for many fish species, including a whole genome assembly of the economically important Nile tilapia, *Oreochromis niloticus* (http://www.ncbi.nlm.nih.gov/genome/197). The ever-increasing availability of DNA sequence data facilitates candidate-gene approaches through comparative genomics by taking advantage of interspecies synteny – the possession of similar chromosomal regions due to common evolutionary descent – to transfer relevant genomic information obtained from studies on well-characterized species to studies involving emerging species (Sarropoulou et al., 2007). One way of identifying synteny between species is to assess the distribution of shared genetic markers in both genomes and identify regions where a common ordering of those

* Corresponding author at: Harte Research Institute, Texas A&M University-Corpus Christi, Corpus Christi, TX 78412, USA. Tel.: +1 361 825 2567; fax: +1 361 825 2025.
E-mail address: christopher.hollenbeck@tamucc.edu (C.M. Hollenbeck).

http://dx.doi.org/10.1016/j.aquaculture.2014.08.045
0044-8486/

markers occurs. Type-I (protein-encoding) genetic markers (O'Brien, 1991) are ideal for this approach as they are often conserved between species, and when incorporated into a linkage map can provide a framework for comparative genomic analysis.

Here, we present a genetic linkage map for red drum, expanding upon previous work (Karlsson et al., 2007; Portnoy et al., 2010, 2011) by the addition of 177 anonymous microsatellites and 46 microsatellites closely linked to Type-I loci. We report the map locations of a total of 486 microsatellites, including the 46 linked to Type-I loci, spanning all 24 (haploid) red drum chromosomes. We also demonstrate the application of the genetic map as a tool for candidate-gene identification through comparative genomics by putatively localizing an additional 80 known (but previously unmapped) red drum protein-encoding genes and microsatellites closely linked to Type-I loci (EST-SSRs), using a synteny-based mapping approach.

2. Materials and methods

In previous studies (Karlsson et al., 2007; Portnoy et al., 2010, 2011), two full-sib mapping families (Family A, $n = 103$; and Family B, $n = 104$), generated from outbred, single-pair crosses carried out at the Marine Development Center of the Texas Parks and Wildlife Department (TPWD), were used. This study took advantage of the same tissue samples used in those studies; details of crosses, spawning, egg collection, and larval grow-out may be found in Portnoy et al. (2010) and references therein.

A total of 177 polymorphic, anonymous microsatellites were isolated from a repeat-enriched library. Details of enriched-library preparation, primer sequences, and summary statistics for each microsatellite can be found in Renshaw et al. (2012). In addition, 133 expressed sequence tag-linked microsatellites (EST-SSRs) were designed following the comparative approach outlined in Hollenbeck et al. (2012). Summary information, including repeat motif, primer sequences, and putative identity for all EST-SSRs are given in Supplementary Table 1. Genomic DNA was extracted following a modified Chelex extraction protocol (Estoup et al., 1996). Following removal of residual Chelex by centrifugation at 16,000 × g, 1 μl of supernatant was used for each PCR reaction, following Portnoy et al. (2010). The 177 anonymous microsatellites and the 46 microsatellites linked to Type-I loci (=223 total) yielded mapping-informative genotypes in at least one parent and were subsequently genotyped in the appropriate progeny. Genotyping was conducted following procedures outlined in Portnoy et al. (2010).

Because individuals genotyped in this study also were used in prior mapping efforts, genotype data from the 223 microsatellites scored here were combined with genotypes at the 264 microsatellites assayed previously by Karlsson et al. (2007) and Portnoy et al. (2010, 2011). Linkage analysis was conducted with the program JoinMap v 4.1 (Van Ooijen, 2012) and linkage groups were defined initially by using microsatellites previously assigned to the 24 red drum linkage groups (Portnoy et al., 2011). New markers were assigned to existing linkage groups, using an LOD threshold of 3.0. Marker order for each linkage group was computed using the maximum-likelihood (ML) mapping function implemented in JoinMap. Tests for segregation distortion for each marker were carried out using a chi-square goodness-of-fit test; probabilities of individual genotypes, conditional upon the map order, were computed to check for possible genotyping errors. A preliminary map was generated for each parent, and marker order was compared between individuals to ensure order agreement. If marker order for each linkage group was in agreement across all parents, a family-specific map was generated using the multipoint ML algorithm for map construction with full-sib outbred families, as implemented in JoinMap and described in van Ooijen (2011). Briefly, the algorithm generates separate ML maps for each parent in a cross, and then integrates the maps by averaging distances between shared intervals and interpolating or extrapolating positions of markers segregating in only one of the parents. Family-specific maps were then checked for marker order agreement. Finally, both family-specific maps were integrated into a consensus map, using the program MergeMap (Wu et al., 2011), which has been demonstrated to produce more accurate consensus maps than JoinMap (Galeano et al., 2011; Wu et al., 2011). In addition, to investigate sex-related differences in recombination rates, female- and male-specific maps were generated using the regression mapping algorithm in JoinMap.

The consensus map was used to compare the red drum genome with assembled genome sequences and chromosome designations of four other fishes: Nile tilapia (*O. niloticus*), three-spined stickleback (*Gasterosteus aculeatus*), green spotted puffer (*Tetraodon nigroviridis*), and Japanese pufferfish (*Takifugu rubripes*). The most recent assembly of each species' genome (Nile tilapia, v 1.1, http://www.ncbi.nlm.nih.gov/genome/197; three-spined stickleback, v 1.0, http://www.ensembl.org/Gasterosteus_aculeatus/Info/Index; green spotted pufferfish, v 8, http://www.ensembl.org/Tetraodon_nigroviridis/Info/Index; Japanese pufferfish, v 5, http://www.ncbi.nlm.nih.gov/genome/63) was downloaded to a Linux server. The discontiguous-megablast algorithm in NCBI's BLAST+ suite (Camacho et al., 2009) was used to compare flanking sequences of the original clone of each mapped red drum microsatellite or EST sequence (for EST-SSRs) with each comparison genome. Clone sequences were available on GenBank for 429 of the 440 mapped anonymous microsatellites; clone sequences of 11 of the anonymous microsatellites were not available. In total, 475 mapped microsatellites (429 anonymous and 46 EST-SSRs) were used in the BLAST search. Matches were considered similar if they had a region of $\geq$50 bp of sequence overlap and had an e-value of $\leq 10^{-10}$. To prevent duplicated sequences from confounding results, only sequences with a single match within a genome were considered for further analysis. Chromosome number and chromosomal position (in base pairs) was recorded for each hit, and Oxford plots comparing the red drum linkage map to the genome of each of the four comparison species were generated, using the GRID graphics package in R (Murrell, 2005). As the comparison species most relevant to aquaculture, Nile tilapia was chosen for a more detailed analysis of synteny with red drum. To visualize the extent of marker collinearity between red drum and Nile tilapia, positions of markers with significant matches to the Nile tilapia genome were coded as relative positions along the length of their respective chromosomes/linkage groups. For Nile tilapia, the start position of the marker, in base pairs, was divided by the total length of the chromosome, in base pairs. For red drum, the position of each marker, in centiMorgans (cM), on the consensus map was divided by the total length of the linkage group, in cM. Based on the observation that the majority of individual red drum linkage groups corresponded to individual Nile tilapia chromosomes, the latter were reorganized along the y-axis such that chromosomes homologous between the two species aligned along the diagonal axis of the graph. Shared markers were then plotted based on their relative positions on linkage groups/chromosomes. A custom Perl script (available upon request from CMH) was used to identify blocks of shared synteny between red drum chromosomes and chromosomes of each of the four comparison species. Syntenic blocks were defined as sets of markers on the same linkage group and in the same order in both species, uninterrupted by any other shared marker. Ordering mismatches between markers that were separated by less than five percent of the total length of a linkage group/chromosome were ignored in order to maximize detection of informative syntenies otherwise disrupted by small-scale, local rearrangements or ordering errors caused by uncertainty in the mapping process. Syntenic regions from chromosomes involved in apparent rearrangements observed from the Oxford plots were plotted as circular ideograms, using the software CIRCOS v 0.66 (Krzywinski et al., 2009).

A synteny-based mapping approach was used to identify likely locations of red drum coding genes that were archived on NCBI's GenBank and of EST-SSRs that were characterized by Hollenbeck et al. (2012) but which were monomorphic in mapping families and could therefore not be mapped via linkage analysis. Nucleotide sequences for 85 red

drum coding genes were downloaded from GenBank and reduced to 72 novel nucleotide sequences by excluding duplicate entries for the same locus. These sequences and the 87 monomorphic EST-SSRs were compared by BLAST search to each of the four comparison genomes, using the same criteria mentioned above. Given that these loci are known to exist in the red drum genome, a locus that maps in another species to a syntenic region shared between red drum and that species likely exists in the same region of the red drum genome. Thus, these loci were mapped to the genomes of the four comparison species, and when red drum genes and EST-SSRs mapped into computed syntenic regions in at least one other species, the locus was putatively localized to that marker interval in red drum.

3. Results

The genetic linkage map constructed for Family A contained 372 microsatellites, including 32 linked to Type-I loci; the map for Family B contained 406 microsatellites, including 34 linked to Type-I loci. The map for Family A had a total size of 1641.2 cM, with an average linkage group size of 68.38 cM and an average marker interval of 4.81 cM; the map for Family B had a total size of 1722.0 cM, with an average linkage group size of 71.75 cM and an average marker interval of 4.55 cM. The consensus map (Fig. 1) contained 486 microsatellites, including 46 linked to Type-1 loci. The total size, average linkage group size, and average marker interval of the consensus map were 1815.3 cM, 75.64 cM, and 3.96 cM, respectively. A single microsatellite, *Soc*685, which was mapped to linkage group eight in a previous study (Portnoy et al., 2010), was removed from the final map due to the presence of significant segregation distortion in all four parents. Of the 46 microsatellites linked to Type-1 loci, 38 (82.6%) could be assigned a putative identity following a BLASTN search of NCBI's nucleotide (nt) database (Supplementary Table 1). Analysis of sex-specific maps in all 24 haploid chromosomes revealed differences in recombination fraction in marker intervals shared between male and female linkage maps (Supplementary Table 2). The overall ratio of recombination fractions for all shared intervals was 1.14:1 (♀:♂).

Of the 429 anonymous microsatellites with available clone sequences, 163 (38.0%) had significant homology to the Nile tilapia genome. Of these, six were excluded from further analysis due to homologies with sequences on multiple chromosomes. A total of 41 (89.1%) of the 46 microsatellites linked to Type I loci showed significant sequence similarity to the Nile tilapia genome; of these, three were excluded due to similarity to regions on multiple chromosomes. The total number of BLAST hits across both microsatellite types was 204 (Nile tilapia), 154 (three-spined stickleback), 105 (Japanese pufferfish), and 84 (green spotted pufferfish).

Oxford plots for all species (Fig. 2) revealed significant homology between red drum linkage groups and chromosomes of the four comparison species, with an approximate one-to-one relationship observed between red drum linkage groups and the chromosomes of each of the species. A number of both intra- and inter-chromosomal rearrangements, however, appear to have occurred since red drum and each of the four comparison

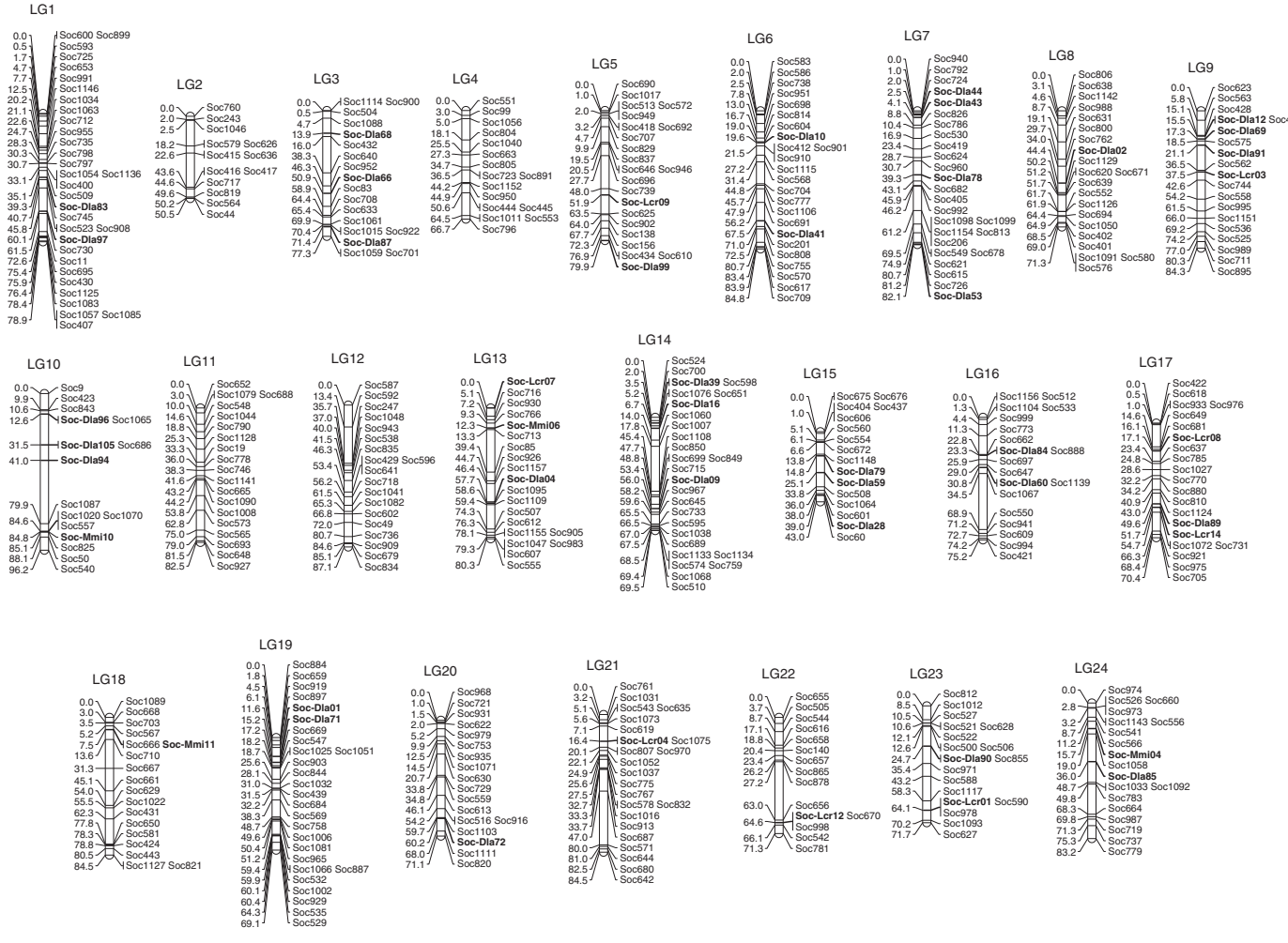

Fig. 1. Consensus genetic linkage map based on segregation in two full-sib families of red drum, *Sciaenops ocellatus*. Map distances, in cM, are given to the left of each linkage group (LG), while marker names are given on the right; marker names in bold represent gene-linked (Type-I) microsatellites.

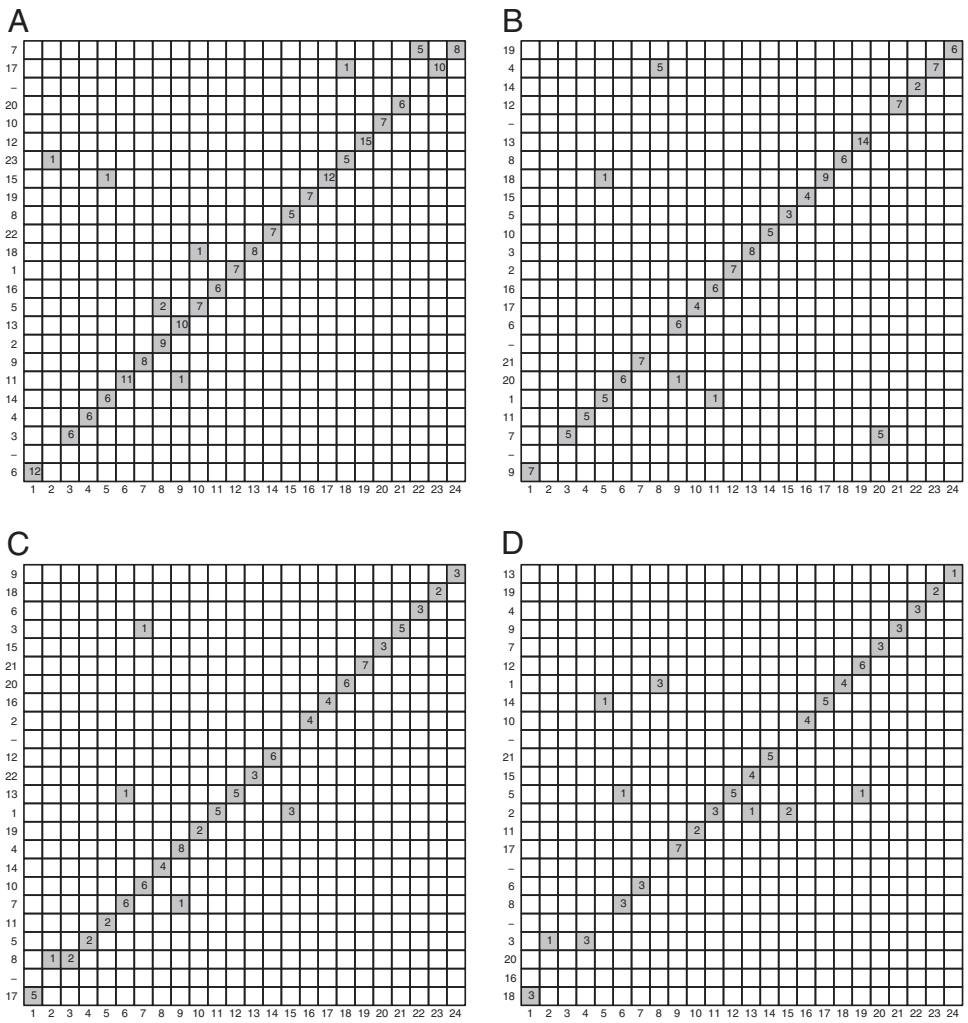

Fig. 2. Oxford plots displaying synteny between linkage groups of red drum and chromosomes of four comparison species. Abscissa: linkage groups 1–24 of red drum; ordinate: chromosomes of comparison species, arranged by homology to linkage groups of red drum. Comparison species are: A, Nile tilapia (*Oreochromis niloticus*); B, three-spined stickleback (*Gasterosteus aculeatus*); C, Japanese pufferfish (*Takifugu rubripes*); and D, green spotted pufferfish (*Tetraodon nigroviridis*). Numbers in grid squares indicate the number of markers (loci) shared between a red drum linkage group and a chromosome in a comparison species.

species diverged from common ancestors. Examples of inferred chromosomal rearrangements, based on shared syntenic group locations, are presented in Fig. 3. Several instances where linkage groups on the same red drum chromosome occurred on more than one chromosome of a comparison species were observed; these included five instances in Nile tilapia and three instances each in the other three comparison species. Finally, a comparison of marker order between putatively homologous chromosomes in red drum and Nile tilapia revealed large regions of synteny and shared marker order between the two species (Fig. 4). Shared markers generally aligned along the diagonal axis of the plot, which is expected if markers are largely collinear.

Based on criteria described above, 47 syntenic regions were identified between red drum and Nile tilapia and a total of 172 microsatellites were placed into syntenic regions. The number of microsatellites per syntenic region ranged from two to ten, with a mean of 3.66. Combined, syntenic regions spanned 306 Mb (46.6%) of the Nile tilapia genome assembly and 838.29 cM (46.2%) of the red drum map. In addition, 33, 30, and 23 syntenic regions were identified between red drum and three-spined stickleback, Japanese pufferfish, and green spotted puffer, respectively; syntenic regions spanned 37.8% (three-spined stickleback), 36.5% (Japanese pufferfish), and 32.1% (green spotted pufferfish) of the species' genome assemblies.

Of the 72 protein-encoding genes in red drum available on GenBank, 50 had a single hit to the genome of at least one of the four comparison species. Of these, 28 (50.6%) were mapped to a genomic interval by synteny-based mapping. Of the 87 monomorphic EST-SSRs in red drum, 79 had a single hit to the genome of at least one of the four comparison species; 52 of these (65.8%) were mapped with the same approach. Fifty of the EST-SSRs were assigned a putative identity based on a BLASTN search of NCBI's nt database. A summary of the 28 protein-encoding genes and the 52 EST-SSRs, including GenBank accession number, putative identity, flanking markers, species in which the syntenic regions are conserved, linkage group in red drum, and estimated genome interval size, is given in Table 1. The map locations of 17 of the coding genes and of 25 of the EST-SSRs were supported by shared synteny in more than one of the four comparison species.

4. Discussion

An additional 227 microsatellites were added to the existing red drum map, increasing the total number of mapped microsatellites to 486 (440 anonymous, 46 linked to Type-I loci). The addition of these microsatellites decreased the inter-marker interval from 6.28 cM (previous sex-averaged map) to 3.96 cM. The total length of the consensus map was 1815.3 cM. This is larger than the size (1196.9 cM) of the sex-averaged map reported previously (Portnoy et al., 2010), for two possible reasons. First, the additional microsatellites sampled more of the chromosomal content of the red drum genome by mapping

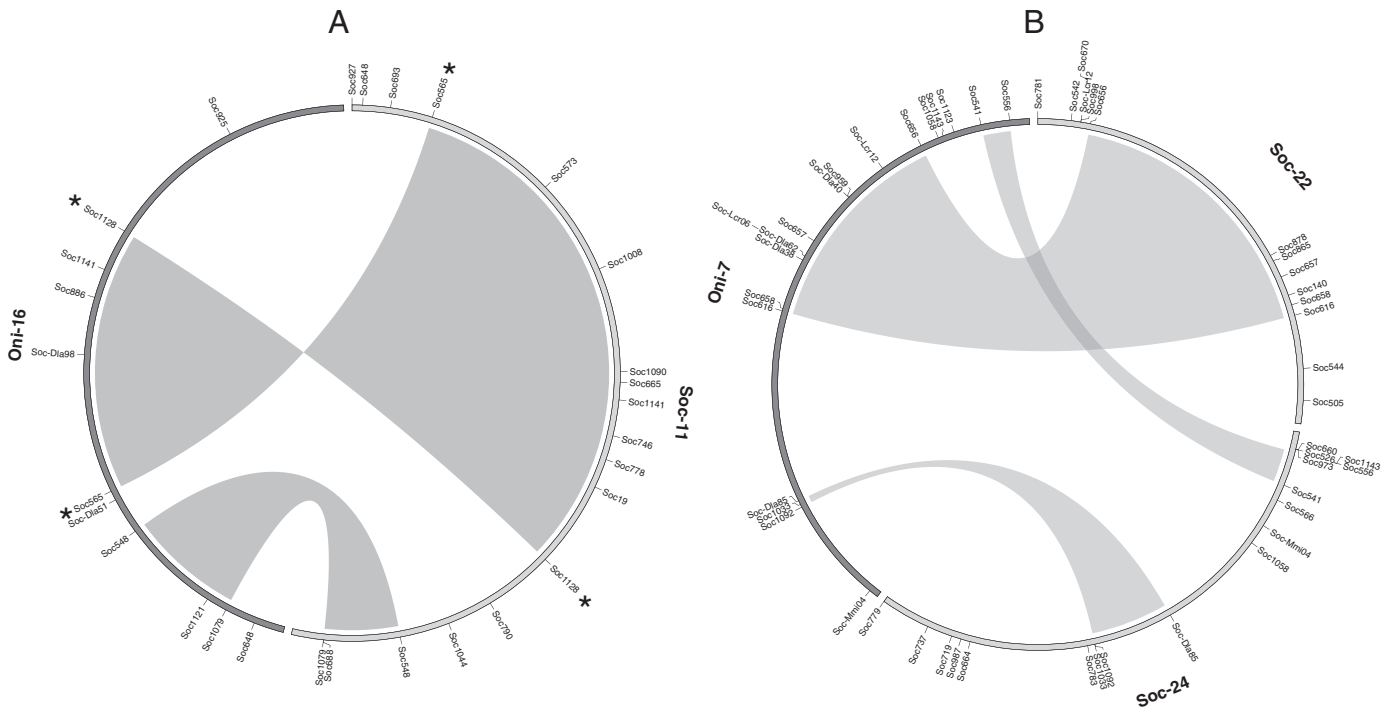

Fig. 3. Circular ideograms, generated using CIRCOS v 0.66, showing putative intra- and inter-chromosomal rearrangements that occurred since red drum and Nile tilapia diverged from a common ancestor. A, an inferred chromosomal rearrangement involving syntenic groups on red drum linkage group 11 (*Soc*-11) and Nile tilapia chromosome 16 (*Oni*-16). Ribbons linking chromosomes represent regions of shared synteny. The two syntenic regions derived from *Soc*-11 are inverted on *Oni*-16 relative to their position on *Soc*-11. Asterisks indicate the ends of relocated syntenic blocks. B, an inferred fusion involving syntenic groups on two red drum chromosomes (*Soc*-22 and *Soc*-24) occurring on a single Nile tilapia chromosome (*Oni*-7). A fusion in the Nile tilapia lineage is inferred because *Soc*-22 and *Soc*-24 are syntenic to separate chromosomes in the other three comparison species (data not shown). The two syntenic regions from *Soc*-24 flank a single syntenic region from *Soc*-22 on *Oni*-7, suggesting that a fusion was followed by one or more intra-chromosomal rearrangements.

locations distal to markers on the previous map; and second, a component of the difference is likely attributable to the process of merging family-based maps into a single consensus map. Because of known differences in recombination rate between sexes in red drum (Portnoy et al., 2010) and differences in marker polymorphism between individual parents, distances between markers in the consensus map may

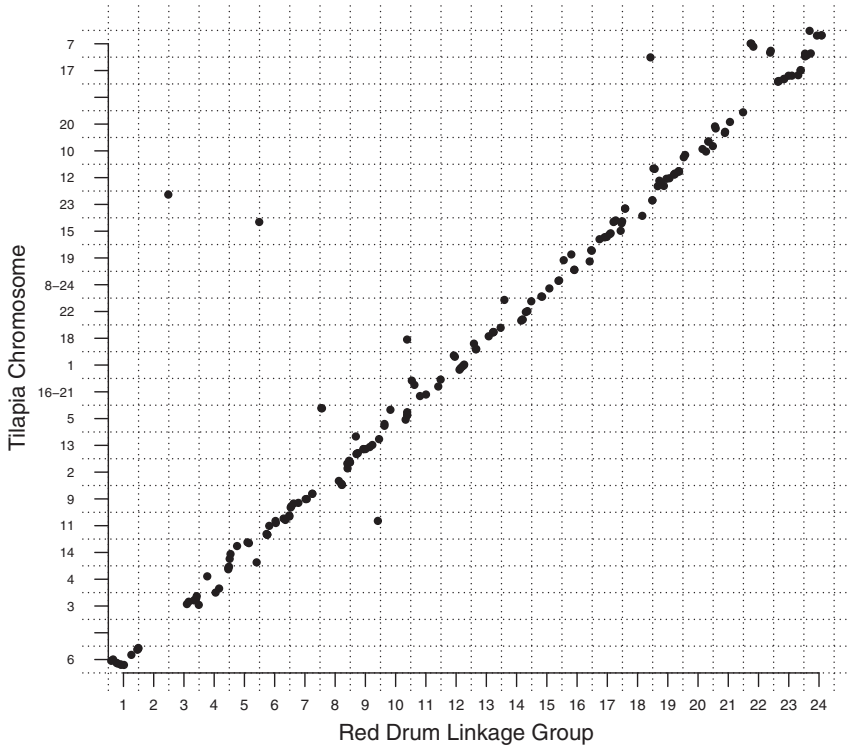

Fig. 4. Comparison of synteny and marker order between markers (loci) shared by red drum and Nile tilapia. Abscissa: linkage groups 1–24 of red drum; ordinate: Nile tilapia chromosomes, arranged by homology, to linkage groups of red drum. Shared markers are plotted relative to their position on a given chromosome/linkage group.

Table 1
Summary of synteny-mapped loci. Accession no. — GenBank accession number of a gene sequence or EST; Function — the assigned gene name from GenBank or a significant BLASTN hit (ESTs); Flanking loci — the closest red drum markers between which the locus from GenBank could be mapped based on synteny with another species; Comparison species — the species in which a syntenic relationship with red drum existed: 1: three-spined stickleback, 2: green spotted puffer, 3: Nile tilapia, 4: fugu; Linkage group — the red drum linkage group to which the locus was mapped; Interval — the size of the corresponding marker interval in centiMorgans on the red drum map.

Accession no.	Putative function	Flanking loci		Comparison species	Linkage group	Interval
Genes						
AF062520.1	*Sciaenops ocellatus* Somatolactin precursor	*Soc*646	*Soc*418	1, 3	5	17.28
AF064872.1	*Sciaenops ocellatus* Translation initiation factor eIF-2B precursor	*Soc*810	*Soc*880	1, 2, 3, 4	17	6.68
AY677170.1	*Sciaenops ocellatus* Salmon-type gonadotropin-releasing hormone precursor	*Soc-Lcr*03	*Soc-Dla*91	1, 3	9	16.4
AY677171.1	*Sciaenops ocellatus* Chicken II-type gonadotropin-releasing hormone precursor	*Soc-Mmi*10	*Soc*1065	1	10	72.2
AY876899.1	*Sciaenops ocellatus* Hemoglobin beta chain	*Soc*1148	*Soc-Dla*28	4	15	25.22
FJ415100.1	*Sciaenops ocellatus* Peptidoglycan recognition protein II	*Soc-Dla*97	*Soc*1125	4	1	16.33
GQ384067.1	*Sciaenops ocellatus* 11 beta-hydroxylase (CYP11B)	*Soc-Dla*10	*Soc*1115	1, 3	6	7.62
GQ384068.1	*Sciaenops ocellatus* 21-hydroxylase (CYP21)	*Soc-Dla*10	*Soc*1115	3	6	7.62
FJ641038.1	*Sciaenops ocellatus* Neuronal nitric oxide synthase	*Soc-Dla*01	*Soc-Dla*71	2, 3, 4	19	3.66
GU144512.1	*Sciaenops ocellatus* Glycoprotein alpha subunit	*Soc*1139	*Soc*550	2, 3	16	38.15
GU144513.1	*Sciaenops ocellatus* Thyrotropin beta subunit	*Soc*1087	*Soc-Dla*96	1, 2	10	67.26
GU799603.1	*Sciaenops ocellatus* Insulin-like growth factor I	*Soc*978	*Soc-Dla*90	2, 4	23	39.33
GU368832.1	*Sciaenops ocellatus* Recombination activating protein 1 (RAG1)	*Soc*719	*Soc*1092	1	24	22.63
GU368812.1	*Sciaenops ocellatus* si:dkey-174m14.3 gene	*Soc*810	*Soc*1072	4	17	13.86
GU370888.1	*Sciaenops ocellatus* ISG15	*Soc*758	*Soc*569	1, 3, 4	19	10.37
GU929942.1	*Sciaenops ocellatus* Viperin (Vip)	*Soc*1139	*Soc*550	2, 3	16	38.15
HM581689.1	*Sciaenops ocellatus* Putative tissue factor pathway inhibitor 1	*Soc*1141	*Soc*1128	4	11	16.33
HM368401.1	*Sciaenops ocellatus* Putative tissue factor pathway inhibitor 2 (TFPI2)	*Soc-Dla*09	*Soc*1108	1	14	10.57
HQ651238.1	*Sciaenops ocellatus* High mobility group protein B1 (HMGB1)	*Soc*949	*Soc*1017	3, 4	5	0.98
HQ731135.1	*Sciaenops ocellatus* FIC domain-containing protein (ficd)	*Soc-Dla*01	*Soc-Dla*71	1, 2, 3, 4	19	3.66
HQ731297.1	*Sciaenops ocellatus* Receptor-interacting serine–threonine kinase 4 (RIPK4)	*Soc-Dla*72	*Soc*820	1, 3	20	10.92
JX002675.1	*Sciaenops ocellatus* Eukaryotic translation initiation factor 3 subunit G (eTIF3)	*Soc*1040	*Soc*804	2, 4	4	7.42
JX002676.1	*Sciaenops ocellatus* NADH dehydrogenase 1 alpha (ND1)	*Soc*1141	*Soc*1128	4	11	16.33
JQ938122.1	*Sciaenops ocellatus* Hypothetical protein (GCS1)	*Soc*991	*Soc*1063	2	1	13.46
JQ938817.1	*Sciaenops ocellatus* Peroxisomal enoyl-CoA hydratase/L-3-hydroxyacyl-CoA dehydrogenase (EHHADH)	*Soc*565	*Soc*1141	1, 3, 4	11	33.45
JQ939810.1	*Sciaenops ocellatus* LOC562320 (KIAA1239)	*Soc-Dla*68	*Soc*640	1, 4	3	24.44
KC830168.1	*Sciaenops ocellatus* Sushi/von Willebrand factor type A/EGF/pentraxin domain-containing 1 (SVEP1)	*Soc-Dla*68	*Soc*640	1	3	24.44
KF140446.1	*Sciaenops ocellatus* T-box brain 1 (tbr1)	*Soc*565	*Soc*1141	1, 3, 4	11	33.45
EST-SSRs						
FP242838.1	*Oreochromis niloticus* Arginine–glutamic acid dipeptide (RE) repeats (rere)	*Soc*1052	*Soc*578	1, 2, 4	21	10.62
FM010232.1	*Neolamprologus brichardi* Calcium/calmodulin-dependent protein kinase type II subunit gamma-like (LOC102781265)	*Soc-Dla*59	*Soc-Dla*79	1, 3	15	10.3
FK943099.1	*Anoplopoma fimbria* Beta-synuclein	*Soc-Dla*02	*Soc*1129	1, 2, 3, 4	8	5.85
FP237559.1	*Neolamprologus brichardi* Guanine nucleotide-binding protein G(s) subunit alpha-like (LOC102788485)	*Soc-Mmi*10	*Soc*1065	1	10	72.2

Table 1 *(continued)*

Accession no.	Putative function	Flanking loci		Comparison species	Linkage group	Interval
FP241017.1	*Maylandia zebra* DNA damage-binding protein 1-like (LOC101485195)	*Soc*718	*Soc*1048	4	12	19.2
FP238020.1	*Oreochromis niloticus* Protein phosphatase 1 regulatory subunit 14B-like (LOC100711861)	*Soc-Dla*66	*Soc*708	1, 3	3	13.45
FL488459.1	*Oreochromis niloticus* Protein-L-isoaspartate (D-aspartate) O-methyltransferase-like (LOC100708432)	*Soc-Lcr*14	*Soc-Dla*89	3, 4	17	2.11
FK941535.1	*Oreochromis niloticus* Elongation of very long chain fatty acids protein 6-like (LOC100706271)	*Soc*694	*Soc*1050	3	8	0.48
CV186185.1	*Danio rerio* si:dkey-11e23.5 (si:dkey-11e23.5)	*Soc*810	*Soc*1072	4	17	13.86
FM028201.1	*Oreochromis niloticus* Phosphatidylserine synthase 1 (ptdss1)	*Soc-Dla*10	*Soc*412	1, 3, 4	6	1.92
FM001773.1	*Oreochromis niloticus* ATPase asna1-like (LOC100702925)	*Soc*991	*Soc*1063	2, 3	1	13.46
FK940504.1	*Haplochromis burtoni* Protein FAM212A-like (LOC102290510)	*Soc*825	*Soc-Mmi*10	1, 3, 4	10	0.25
FM000143.1	*Maylandia zebra* Prospero homeobox protein 1-like (LOC101476671)	*Soc*810	*Soc*880	1, 2, 3, 4	17	6.68
FM023318.1	*Oreochromis niloticus* Thioredoxin reductase 3 (txnrd3)	*Soc*423	*Soc-Dla*96	1	10	2.69
FM027384.1	*Neolamprologus brichardi* AF4/FMR2 family member 4-like (LOC102796839)	*Soc*630	*Soc*1071	2, 4	20	6.16
FM004496.1	*Oreochromis niloticus* Disco-interacting protein 2 homolog B-A-like (LOC100703539)	*Soc*1052	*Soc*578	1, 2, 4	21	10.62
FM009184.1	*Neolamprologus brichardi* Hippocalcin-like protein 1-like (LOC102792629)	*Soc-Dla*09	*Soc*849	3	14	7.16
FM011451.1	*Haplochromis burtoni* Myristoylated alanine-rich C-kinase substrate-like (LOC102308505)	*Soc*975	*Soc*921	3	17	2.07
FM000141.1	*Oreochromis niloticus* Junction plakoglobin-like (LOC100707214)	*Soc*430	*Soc-Dla*97	1, 3	1	15.84
FK940790.1	*Oreochromis niloticus* Serine-rich coiled-coil domain-containing protein 2-like (LOC100710988)	*Soc-Lcr*03	*Soc-Dla*91	1	9	16.4
FM010695.1	*Neolamprologus brichardi* Neurotrypsin-like (LOC102780776)	*Soc-Dla*59	*Soc*1148	3	15	11.33
FM012479.1	*Neolamprologus brichardi* MAP7 domain-containing protein 1-like (LOC102788526)	*Soc*1133	*Soc*645	3	14	8.82
AM986102.1	*Oreochromis niloticus* Protein bicaudal D homolog 2-like (LOC100712336)	*Soc*642	*Soc*687	3	21	37.51
FM000541.1	*Haplochromis burtoni* Notch-regulated ankyrin repeat-containing protein A-like (LOC102310701)	*Soc*657	*Soc*658	3	22	4.65
FP238879.1	*Haplochromis burtoni* Mucin-17-like (LOC102294623)	*Soc-Lcr*12	*Soc*657	1, 3	22	41.12
FN565801.1	*Oreochromis niloticus* CCAAT/enhancer-binding protein beta-like (LOC100689715)	*Soc*642	*Soc*687	3	21	37.51
FM013092.1	*Pundamilia nyererei* Lysophospholipid acyltransferase 5-like (LOC102193954)	*Soc*1115	*Soc*777	1, 3	6	18.5
AM987101.1	*Oreochromis niloticus* LIM domain-binding protein 3-like (LOC100707522)	*Soc-Dla*59	*Soc-Dla*79	1, 3	15	10.3
FP237257.1	*Haplochromis burtoni* arf-GAP with dual PH domain-containing protein 1-like (LOC102311544)	*Soc-Dla*79	*Soc-Dla*28	2, 4	15	24.19
FM018821.1	*Oreochromis niloticus* Ubiquitin specific peptidase 9, X-linked (usp9x), transcript variant X7	*Soc*1128	*Soc*548	1	11	15.24
FP242802.1	*Oreochromis niloticus* Calsyntenin-3-like (LOC100707828)	*Soc*1115	*Soc*777	1, 3	6	18.5
FM006783.1	*Oreochromis niloticus* cAMP-dependent protein kinase type I-alpha regulatory subunit-like (LOC100711171)	*Soc-Dla*28	*Soc*601	3	15	0.99
FM017384.1	*Oreochromis niloticus* Beta-14-galactosyltransferase 5-like (LOC100696774)	*Soc*578	*Soc*687	2	21	14.27
AM985524.1	*Neolamprologus brichardi* Dedicator of cytokinesis protein 8-like (LOC102793453)	*Soc-Dla*71	*Soc*439	4	19	16.31
FM007039.1	*Oreochromis niloticus* Zinc finger CCCH domain-containing protein 7B-like (LOC100698451)	*Soc-Dla*79	*Soc-Dla*28	2, 4	15	24.19
FM007045.1	*Haplochromis burtoni* Breakpoint cluster region protein-like (LOC102292921)	*Soc*657	*Soc*658	3	22	4.65

(continued on next page)

Table 1 *(continued)*

Accession no.	Putative function	Flanking loci		Comparison species	Linkage group	Interval
FM012644.1	*Neolamprologus brichardi* Forkhead box protein O3-like (LOC102783221)	*Soc*1072	*Soc*921	4	17	11.57
FM012811.1	*Oreochromis niloticus* Beta-14-galactosyltransferase 5-like (LOC100696774)	*Soc*578	*Soc*687	2	21	14.27
FM021649.1	*Neolamprologus brichardi* E3 ubiquitin-protein ligase MSL2-like (LOC102797866)	*Soc*1139	*Soc*550	2, 3	16	38.15
FM008475.1		*Soc*1117	*Soc*588	3	23	15.03
FM013106.1	*Neolamprologus brichardi* Calcipressin-3-like (LOC102786199)	*Soc*1139	*Soc*550	3	16	38.15
FM000627.1	*Haplochromis burtoni* Nuclear factor 1 X-type-like (LOC102293245)	*Soc*991	*Soc*1063	2	1	13.46
AM984068.1	*Oreochromis niloticus* Cordon-bleu protein-like 1-like (LOC100702457)	*Soc*565	*Soc*1141	1, 3, 4	11	33.45
CX348550.1	*Oryzias latipes* Basic leucine zipper transcriptional factor ATF-like (LOC101168259)	*Soc*810	*Soc*880	1, 2, 3, 4	17	6.68
CX348556.1	*Oreochromis niloticus* Basic leucine zipper transcriptional factor ATF-like (LOC100690329)	*Soc*810	*Soc*880	1, 2, 3, 4	17	6.68
C48612.1	*Haplochromis burtoni* Breakpoint cluster region protein-like (LOC102292921)	*Soc*657	*Soc*658	3	22	4.65
EV413959.1	*Morone saxatilis* Clone apoa1_3 apolipoprotein A-I (ApoA1)	*Soc-Lcr*09	*Soc*646	3	5	31.36
GW668767.1		*Soc*588	*Soc*971	3	23	7.79
GW668773.1	*Maylandia zebra* Basic leucine zipper transcriptional factor ATF-like (LOC101468837)	*Soc*810	*Soc*880	1, 2, 3, 4	17	6.68
GW670899.1	*Oreochromis niloticus* Nuclear factor erythroid 2-related factor 1-like (LOC100705427)	*Soc*850	*Soc*1108	1, 3, 4	14	2.28
GW671772.1	*Neolamprologus brichardi* Nuclear receptor subfamily 2 group F member 6-like (LOC102781642)	*Soc*1095	*Soc*507	1, 3, 4	13	15.69
GW672302.1	*Epinephelus coioides* CCAAT/enhancer-binding protein beta 2	*Soc*642	*Soc*687	3	21	37.51

reflect that of a single individual. If a marker is only segregating in one sex, marker intervals involving that locus in the consensus map will not be a sex-averaged distance, but will reflect only the recombination rate in that particular sex (which could be larger or smaller than the sex-average). In addition, while the software MergeMap outperforms JoinMap in estimating a merged marker order (Galeano et al., 2011; Wu et al., 2011), it also inflates inter-marker distance when combining maps (Khan et al., 2012). However, there exists a tradeoff between accurate estimation of map distances and combining incomplete information from multiple individuals into a single map. For purposes of synteny analysis, establishing the linear order of the maximum number of loci is potentially more useful than having more accurate map distances.

While QTL mapping was not the intention of this study, the linkage map will provide useful information for future QTL mapping studies. For example, the presence of sex-specific differences in recombination fractions between loci should be taken into account in future QTL mapping or marker-assisted selection experiments. Analysis of differences in recombination rates between the sex-specific maps supported the conclusions of Portnoy et al. (2010), in which large differences were observed in specific chromosomal regions, but the overall ratio of recombination rates was near unity, with slightly higher recombination in females (1.03:1 — Portnoy et al., 2010; 1.14:1 — present study).

The addition of 46 microsatellites linked to Type-I loci to the red drum map is important, as a large percentage of mapped Type-I loci (82.6%) were assigned a putative function. Further, an appreciably larger percentage of microsatellites linked to Type-I loci, relative to anonymous microsatellites (89.1% vs. 38.0%), were conserved between red drum and Nile tilapia, demonstrating the utility of microsatellites linked to Type-I loci for comparative genomics analysis. A comparison of the red drum linkage map to the genomes of four different percomorph fishes revealed considerable synteny and that numerous chromosomal rearrangements had occurred since red drum and each of the comparison species last shared a common ancestor. While a one-to-one chromosomal relationship generally was observed between red drum linkage groups and chromosomes of each of the four comparison species, there were several instances where regions from different red drum chromosomes were found on a single chromosome of a comparison species, and there were several inferred intra- and inter-chromosomal rearrangements. Overall, the findings are consistent with previous comparative genomics studies in teleost fishes where instances of chromosomal repatterning, as well as a large degree of conserved synteny, have been observed (Kucuktas et al., 2009; Sarropoulou et al., 2007).

The comparatively high degree of synteny, in terms of total number of syntenic regions, number of loci present in those regions, and percent of genome assembly covered by syntenic regions, between red drum and Nile tilapia was not unexpected. The red drum EST-SSRs were designed by using a comparative approach that utilized an unassembled version of the Nile tilapia genome to ensure maximum cross-species amplification (Hollenbeck et al., 2012), and red drum (Family Sciaenidae; Order Perciformes) and Nile tilapia (Family Cichlidae; Order Perciformes) are regarded as closer phylogenetically than red drum is to either sticklebacks (Order Gasterosteiformes) or Japanese and green spotted pufferfish (Order Tetraodontiformes) (Nelson, 2006). The high degree of synteny and conservation of marker order between red drum and Nile tilapia may be useful in future genetic mapping of QTL in red drum. Tilapias, *Oreochromis* spp., have been the subject of considerable genetics research related to aquaculture, and QTL influencing production-relevant traits (e.g., growth rate, immune and stress response, sex determination, cold tolerance) have been identified (Cnaani et al., 2003, 2004; Lee et al., 2003, 2004; Moen et al., 2004; Shirak et al., 2006). Based on the current set of loci shared between the two species, 47 syntenic blocks spanning 306 Mb (46.6% of the Nile tilapia genome assembly) were identified and represent chromosomal regions that have remained intact over evolutionary time and likely

share a significant proportion of homologous genes. Further work to identify these homologous genes in red drum will soon be underway.

Using the syntenic regions identified from all comparisons, it was possible to putatively localize an additional 28 red drum protein-encoding genes (whose sequences were annotated by means of high homology to sequences in GenBank) and 52 unmapped EST-SSRs to marker intervals on the red drum map. The 28 coding genes taken from GenBank are of practical interest as some appear to be involved in immune response. These include: (i) the neuronal nitric oxide synthase (nNOS) gene, which is expressed in a number of tissues and thought to be involved in innate immune response (Zhou et al., 2009); (ii) the high mobility group protein B1 (HMGB1), which is up-regulated in response to bacterial challenge and is thought to be involved in immune function (Zhao et al., 2011); and (iii) the product of the tissue factor pathway inhibitor 2 gene (TFPI-2), which is thought to play a role in the response to bacterial infection (Zhang and Sun, 2011). In addition, 50 of 52 synteny-mapped EST-SSRs could be assigned a putative function following a BLASTN search. These include a gene coding for a thioredoxin reductase protein, which has been shown to be expressed during pathogen infection in rainbow trout (Pacitti et al., 2014), and a gene encoding a junction plakoglobin gene product, which has been observed to be upregulated in channel catfish skin tissue in response to pathogen challenge (Li et al., 2013).

In summary, the current linkage map of 486 total microsatellites (440 anonymous, 46 gene-linked) proved a powerful tool for comparative genomics. Using synteny-based mapping, we putatively localized an additional 28 red drum protein-encoding genes and 52 red drum EST-SSRs. The mapping of highly conserved anchor loci will provide a framework for future comparative work and should allow researchers to utilize relevant genomic information from studies involving well-characterized species to inform candidate-gene approaches to QTL detection in red drum. The general strategy presented for mapping by synteny can be applied to any species without an available genome assembly, but with an available linkage map. In addition, the map potentially will facilitate identification of chromosomal regions under the influence of natural selection in wild populations of red drum, and in this way could inform both management of wild stocks and stock-enhancement decisions. Moreover, the genetic map will be a valuable resource for future genomics research in red drum, including physical mapping and genome assembly.

Supplementary data to this article can be found online at http://dx.doi.org/10.1016/j.aquaculture.2014.08.045.

Acknowledgments

We thank R. Vega and R. Gamez of the TPWD Marine Development Center in Corpus Christi, TX, for their assistance with crosses and sampling, M. Renshaw for help in the laboratory, J. Puritz for helpful comments on the manuscript, and the Editor and three anonymous reviewers for helpful comments on the manuscript. Work was supported by Award # NA10NMF4270199 of the Saltonstall-Kennedy Program of the National Marine Fisheries Service (National Oceanic and Atmospheric Administration), Award # NA10OAR4170099 from the National Oceanic and Atmospheric Administration to Texas Sea Grant, the Coastal Fisheries Division of the Texas Parks and Wildlife Department, and Texas AgriLife Project H-6703. This paper is number 100 in the series 'Genetic Studies in Marine Fishes.' and contribution number 6 of the Marine Genomics Laboratory.

References

Camacho, C., Coulouris, G., Avagyan, V., Ma, N., Papadopoulos, J., Bealer, K., Madden, T.L., 2009. BLAST+: architecture and applications. BMC Bioinf. 10, 421. http://dx.doi.org/10.1186/1471-2105-10-421.

Cnaani, A., Hallerman, E., Ron, M., Weller, J., 2003. Detection of a chromosomal region with two quantitative trait loci, affecting cold tolerance and fish size, in an F_2 tilapia hybrid. Aquaculture 223, 117–128.

Cnaani, A., Zilberman, N., Tinman, S., Hulata, G., Ron, M., 2004. Genome-scan analysis for quantitative trait loci in an F_2 tilapia hybrid. Mol. Genet. Genomics 272, 162–172. http://dx.doi.org/10.1007/s00438-004-1045-1.

Danzmann, R.G., Gharbi, K., 2007. Linkage mapping in aquaculture species. In: Liu, Z. (Ed.), Aquaculture Genome Technologies. Blackwell Publishing Ltd., Oxford, UK, p. 551.

Estoup, A., Largiader, C.R., Perrot, E., Chourrout, D., 1996. Rapid one-tube DNA extraction for reliable PCR detection of fish polymorphic markers and transgenes. Mol. Mar. Biol. Biotechnol. 5, 295–298.

Falconer, D.S., Mackay, T.F.C., 1996. Introduction to Quantitative Genetics, 4th ed. Pearson Education Limited, Harlow, England.

Galeano, C.H., Fernandez, A.C., Franco-Herrera, N., Cichy, K.A., McClean, P.E., Vanderleyden, J., Blair, M.W., 2011. Saturation of an intra-gene pool linkage map: towards a unified consensus linkage map for fine mapping and synteny analysis in common bean. PLoS One 6, e28135. http://dx.doi.org/10.1371/journal.pone.0028135.

Gjedrem, T., Robinson, N., Rye, M., 2012. The importance of selective breeding in aquaculture to meet future demands for animal protein: a review. Aquaculture 350–353, 117–129. http://dx.doi.org/10.1016/j.aquaculture.2012.04.008.

Hollenbeck, C.M., Portnoy, D.S., Gold, J.R., 2012. Use of comparative genomics to develop EST-SSRs for red drum (*Sciaenops ocellatus*). Mar. Biotechnol. 14, 672–680. http://dx.doi.org/10.1007/s10126-012-9449-0.

Hong, W., Zhang, Q., 2003. Review of captive bred species and fry production of marine fish in China. Aquaculture 227, 305–318.

Hulata, G., 2001. Genetic manipulations in aquaculture: a review of stock improvement by classical and modern technologies. Genetica 111, 155–173.

Karlsson, S., Ma, L., Saillant, E., Gold, J., 2007. Tests of Mendelian segregation and linkage-group relationships among 31 microsatellite loci in red drum, *Sciaenops ocellatus*. Aquac. Int. 15, 383–391.

Khan, M.A., Han, Y., Zhao, Y.F., Troggio, M., Korban, S.S., 2012. A multi-population consensus genetic map reveals inconsistent marker order among maps likely attributed to structural variations in the apple genome. PLoS One 7, e47864. http://dx.doi.org/10.1371/journal.pone.0047864.

Krzywinski, M., Schein, J., Birol, I., 2009. Circos: an information aesthetic for comparative genomics. Genome Res. 19, 1639–1645.

Kucuktas, H., Wang, S., Li, P., He, C., Xu, P., Sha, Z., Liu, H., Jiang, Y., Baoprasertkul, P., Somridhivej, B., Wang, Y., Abernathy, J., Guo, X., Liu, L., Muir, W., Liu, Z., 2009. Construction of genetic linkage maps and comparative genome analysis of catfish using gene-associated markers. Genetics 181, 1649–1660. http://dx.doi.org/10.1534/genetics.108.098855.

Leder, E., Danzmann, R., Ferguson, M., 2006. The candidate gene, Clock, localizes to a strong spawning time quantitative trait locus region in rainbow trout. J. Hered. 97, 74–80.

Lee, B., Penman, D., Kocher, T., 2003. Identification of a sex-determining region in Nile tilapia (*Oreochromis niloticus*) using bulked segregant analysis. Anim. Genet. 34, 379–383.

Lee, B.-Y., Hulata, G., Kocher, T.D., 2004. Two unlinked loci controlling the sex of blue tilapia (*Oreochromis aureus*). Heredity (Edinb) 92, 543–549. http://dx.doi.org/10.1038/sj.hdy.6800453.

Li, C., Wang, R., Su, B., Luo, Y., Terhune, J., Beck, B., Peatman, E., 2013. Evasion of mucosal defenses during *Aeromonas hydrophila* infection of channel catfish (*Ictalurus punctatus*) skin. Dev. Comp. Immunol. 39, 447–455. http://dx.doi.org/10.1016/j.dci.2012.11.009.

Liu, Z., Cordes, J., 2004. DNA marker technologies and their applications in aquaculture genetics. Aquaculture 238, 1–37.

Loukovitis, D., Sarropoulou, E., 2012. Quantitative trait loci for body growth and sex determination in the hermaphrodite teleost fish *Sparus aurata* L. Anim. Genet. 43, 753–759.

Lynch, M., Walsh, B., 1998. Genetics and Analysis of Quantitative Traits, 1st ed. Sinauer Associates, Sunderland, MA.

McEachron, L.W., McCarty, C.E., Vega, R.R., 1995. Beneficial uses of marine fish hatcheries: enhancement of red drum in Texas coastal waters. American Fisheries Society Symposium, pp. 161–166.

Moen, T., Agresti, J., Cnaani, A., 2004. A genome scan of a four-way tilapia cross supports the existence of a quantitative trait locus for cold tolerance on linkage group 23. Aquac. Res. 35, 893–904.

Murrell, P., 2005. R Graphics. CRC Press.

Nelson, J.S., 2006. Fishes of the World, 4th ed. John Wiley & Sons, Hoboken, NJ.

O'Brien, S., 1991. Mammalian genome mapping: lessons and prospects. Curr. Opin. Genet. Dev. 1, 105–111.

Pacitti, D., Wang, T., Martin, S.A.M., Sweetman, J., Secombes, C.J., 2014. Insights into the fish thioredoxin system: expression profile of thioredoxin and thioredoxin reductase in rainbow trout (*Oncorhynchus mykiss*) during infection and in vitro stimulation. Dev. Comp. Immunol. 42, 261–277. http://dx.doi.org/10.1016/j.dci.2013.09.013.

Pattillo, M., Czapla, T., Nelson, D., Monaco, M., 1997. Distribution and abundance of fishes and invertebrates in Gulf of Mexico estuaries, Volume II: Species life history summaries. OAA/NOS Strategic Environmental Assessments Division, Rockville, MD.

Portnoy, D.S., Renshaw, M.A., Hollenbeck, C.M., Gold, J.R., 2010. A genetic linkage map of red drum, *Sciaenops ocellatus*. Anim. Genet. 41, 630–641. http://dx.doi.org/10.1111/j.1365-2052.2010.02059.x.

Portnoy, D.S., Hollenbeck, C.M., Renshaw, M.A., Gold, J.R., 2011. Microsatellite panels for gene localization in red drum, *Sciaenops ocellatus*. Aquaculture 319, 505–508. http://dx.doi.org/10.1016/j.aquaculture.2011.06.006.

Renshaw, M.A., Hollenbeck, C.M., Gold, J.R., 2012. Isolation of microsatellite markers from red drum, *Sciaenops ocellatus*, and characterization in red drum and spotted seatrout, *Cynoscion nebulosus*. Mol. Ecol. Resour. 1–22.

Sánchez-Molano, E., Cerna, A., Toro, M.A., Bouza, C., Hermida, M., Pardo, B.G., Cabaleiro, S., Fernández, J., Martínez, P., 2011. Detection of growth-related QTL in turbot (*Scophthalmus maximus*). BMC Genomics 12, 473. http://dx.doi.org/10.1186/1471-2164-12-473.

Sarropoulou, E., Franch, R., Louro, B., Power, D.M., Bargelloni, L., Magoulas, A., Senger, F., Tsalavouta, M., Patarnello, T., Galibert, F., Kotoulas, G., Geisler, R., 2007. A gene-based radiation hybrid map of the gilthead sea bream *Sparus aurata* refines and exploits conserved synteny with *Tetraodon nigroviridis*. BMC Genomics 8, 44. http://dx.doi.org/10.1186/1471-2164-8-44.

Shirak, A., Seroussi, E., Cnaani, A., Howe, A.E., Domokhovsky, R., Zilberman, N., Kocher, T.D., Hulata, G., Ron, M., 2006. Amh and Dmrta2 genes map to tilapia (*Oreochromis* spp.) linkage group 23 within quantitative trait locus regions for sex determination. Genetics 174, 1573–1581. http://dx.doi.org/10.1534/genetics.106.059030.

Smith, T.I.J., Jenkins, W.E., Denson, M.R., Collins, M.R., 2001. Stock enhancement research with anadromous and marine fishes in South Carolina. Ecol. Aquac. Species Enhanc. Stock 175.

Sonesson, A., 2007. Possibilities for marker-assisted selection in aquaculture breeding schemes. In: Guimarães, E.P., Ruane, J., Scherf, B., Sonnino, A., Dargie, J. (Eds.), Marker-Assisted Selection: Current Status and Future Perspectives in Crops, Livestock, Forestry, and Fish. FAO, Rome.

Tao, W.J., Boulding, E.G., 2003. Associations between single nucleotide polymorphisms in candidate genes and growth rate in Arctic charr (*Salvelinus alpinus* L.). Heredity (Edinb) 91, 60–69. http://dx.doi.org/10.1038/sj.hdy.6800281.

Tringali, M.D., Leber, K.M., Halstead, W.G., McMichael, R., O'Hop, J., Winner, B., Cody, R., Young, C., Neidig, C., Wolfe, H., et al., 2008. Marine stock enhancement in Florida: a multi-disciplinary, stakeholder-supported, accountability-based approach. Rev. Fish. Sci. 16, 51–57.

Van Ooijen, J.W., 2011. Multipoint maximum likelihood mapping in a full-sib family of an outbreeding species. Genet. Res. (Camb) 93, 343–349. http://dx.doi.org/10.1017/S0016672311000279.

Van Ooijen, J.W., 2012. JoinMap 4.1. Software for the calculation of genetic linkage maps in experimental populations of diploid species. Softw. Calc. Genet. Link. maps Exp. Popul. Kyazma BV, Wageningen, Netherlands.

Woodward, A.G., 2000. Red drum stock enhancement in Georgia: a responsible approach. Coast. Resour. Div. Georg. Dep. Nat. Resour. Brunswick, GA.

Wu, Y., Close, T.J., Lonardi, S., 2011. Accurate construction of consensus genetic maps via integer linear programming. IEEE/ACM Trans. Comput. Biol. Bioinform. 8, 381–394. http://dx.doi.org/10.1109/TCBB.2010.35.

Zhang, M., Sun, L., 2011. The tissue factor pathway inhibitor 1 of *Sciaenops ocellatus* possesses antimicrobial activity and is involved in the immune response against bacterial infection. Dev. Comp. Immunol. 35, 247–252.

Zhao, L., Hu, Y.-H., Sun, J.-S., Sun, L., 2011. The high mobility group box 1 protein of *Sciaenops ocellatus* is a secreted cytokine that stimulates macrophage activation. Dev. Comp. Immunol. 35, 1052–1058. http://dx.doi.org/10.1016/j.dci.2011.03.025.

Zhou, L., Bai, R., Tian, J., Liu, X., Lu, D., Zhu, P., Liu, Y., Zeng, L., Luo, W., Zhang, Y., Wang, A., 2009. Bioinformatic comparisons and tissue expression of the neuronal nitric oxide synthase (nNOS) gene from the red drum (*Sciaenops ocellatus*). Fish Shellfish Immunol. 27, 577–584. http://dx.doi.org/10.1016/j.fsi.2009.07.010.